Project Acronym:	Hydroptics
Grant Agreement number:	871529 (H2020-ICT-2019-2)
Project Full Title:	Photonics sensing platform for process optimisation in the oil industry

DELIVERABLE

D8.3 – Report on successful pilot II completion

Dissemination level	PU – Public
Type of Document	Report
Contractual date of delivery	30/11/2023
Deliverable Leader	Ekin Meşe (TUPRAS)
Status & version	V2.0
WP / Task responsible	WP8 / TUPRAS
Keywords:	Validation, field test, Hydroptics platform

Deliverable Leader:	TUPRAS
Contributors:	Ahmet Coşgun (TUPRAS) Ekin Meşe (TUPRAS) Işıl Kabacaoğlu (TUPRAS) Bengü Yılmaz (TUPRAS) Dominik Wacht (TUW) Felix Frank (TUW)
Reviewers:	David Gachet (ALPES)
Approved by:	David Gachet (ALPES)

Document History			
Version	**Date**	**Contributor(s)**	**Description**
V1.0	21/12/2023	TUPRAS, TUW	First complete version
V1.1	21/12/2023	ALPES	Minor editing
V2.0	21/12/2023	ALPES	Final version, after review by the Coordinator

1. Executive Summary

This deliverable describes the work done within Task 8.3 “Pilot II – TUPRAS Pilot (Turkey)”. The capability of an IR-based at-line analyzer to give information on the source of oil leaks in a refinery was demonstrated at TUPRAS R&D Center facilities.

The samples gathered from different refinery plants and streams are analyzed in the IR-based at-line analyzer, and the characteristics of these oil samples are discussed for oil in water (OiW) quality analysis. Effective regions are determined for hydrocarbon samples and their differences in spectrometric images are gathered. Overall, the capabilities of potential on-line oil in water analysis, as demonstrated in the Pilot I phase, coupled with tunable infrared spectroscopy, as demonstrated in this Pilot II phase, can be used in the future to quickly react to leaks in the cooling water system, reducing down-time and improving efficiency.

On the other hand, the field testing of TUPRAS water samples with the HYDROPTICS platform is performed at OMV premises for OiW quantity analysis, as part of D8.2.

2. Table of Contents

3. Introduction

One of the main goals of the HYDROPTICS projects is not only to develop a measurement platform, but also to perform the assessment of functionality and figures of merit in real industry settings at the sites of the two industrial partners OMV and TUPRAS. Work package WP8 “Hydroptics sensor validation in real industry settings & Process optimization” was set up for this purpose. Within this work package, tasks T8.2 and T8.3 contain the two planned pilot tests at the sites of OMV and TUPRAS, respectively.

For this purpose, HYDROPTICS platform prototype demonstration was held at OMV premises. TUPRAS water samples, representative of cooling water used in downstream refinery operations, were tested, and observations were made for a real-life environment to ensure functionality beyond standard conditions.

In the Pilot II phase, the capability of an IR-based at-line analyzer to give information on oil leaks in downstream refinery operations was demonstrated at the premises of TUPRAS. For this, the two spectral regions, as defined in the early stages of the project (1,360-1,410 cm^{-1} and 1,470-1,520 cm^{-1}), gave valuable information on the type of products measured. A limit of detection (LOD) of ~80 ppm in Cyclohexane was measured, which would equate to an LOD of 5 ppm in Oil in water, considering an extraction factor of 18. The capabilities of potential on-line OiW analysis, as demonstrated in the Pilot I phase, coupled with tunable infrared spectroscopy, as demonstrated in this Pilot II phase, may be used to quickly identify, and react to leaks in the cooling water system, reducing down-time and improving efficiency.

4. Pilot II – TUPRAS Pilot (Turkey)

4.1. Initial concept

The process in which the analyzer was used in Pilot II is different from the process in Pilot I. In Pilot II, the analyzer was installed in the cooling tower that returns process water. In refinery downstream operations, cooling water systems operate to chill water heated in the process and to recirculate it in the refinery. The main concerns with the quality of cooling water are acidity, conductivity, inorganic ion concentrations, as well as particle and oil amounts. OiW causes microbiological organism formation, corrosion in pipelines and equipment, and risk of flammability. Therefore, it is important to monitor and quickly react to potential oil leaks in the cooling water system to reduce down-time and to improve efficiency. The HYDROPTICS platform solves this problem as an on-line OiW analyzer with both qualitative and quantitative capabilities.

4.2. Sample selection and preparatory work

Oil leakages from hydrocarbon streams to water can occur in different areas in the process industries. One example is the cooling water system, where water is passed through heat exchangers to chill the hydrocarbon products. However, due to possible corrosion**,** leakages can occur. It is important to identify and monitor leakages as fast as possible, and identify points of leakage. Unfortunately, it is often a difficult task, as the water stream passes through numerous heat exchangers in a cooling water system.

The return stream of cooling water to the cooling tower was selected for the HYDROPTICS pilot. A schematic of the process and the tie in point for the pilot are shown in **Figure 1**.

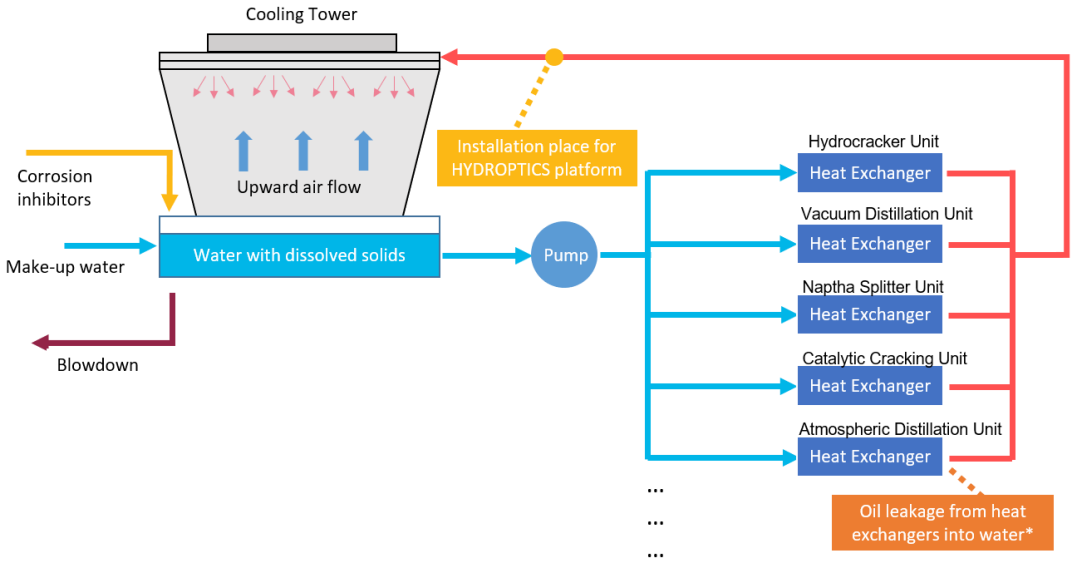

Figure 1: Schematic of the colling water circuit at Tüpraş Izmit Refinery and the planned tie in point for the HYDROPTICS pilot II.

To estimate and point out the candidate leak points, the characteristics of the leaked oil samples had to be studied. To this end, different hydrocarbon samples from TUPRAS were gathered from different products and different plants. The schematic of the sample points are shown in **Figure 2** (in red font).

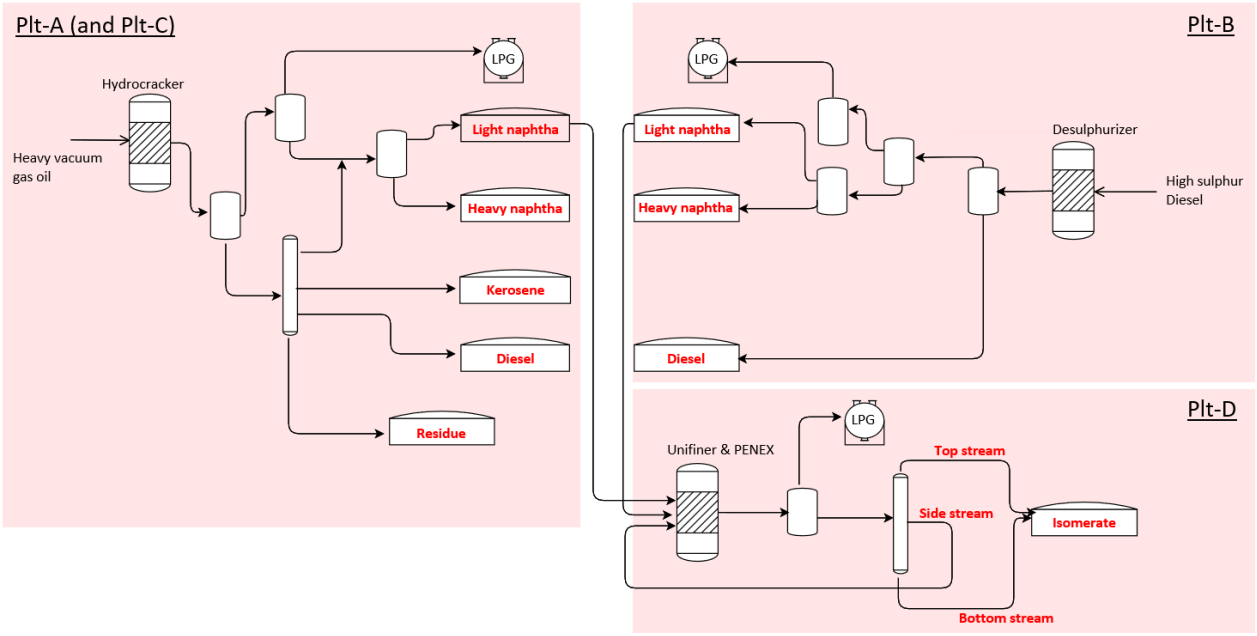

Figure 2: Schematic of the sample points (shown in red font) of TUPRAS samples studied in the HYDROPTICS project.

4.3. Results

4.3.1. Benchmarking the analyzer sensitivity

To identify potential leakages as fast as possible, a low limit of detection (LOD) is necessary for the analyzer. To determine this parameter, a calibration series of 6 concentrations between 1,000 ppm and 6,000 ppm in cyclohexane of an aromatic-rich product was performed. The spectra of the different concentrations of the product are shown in **Figure 3**. Due to the strong absorption of CH_2 in the solvent, the region between 1,480 and 1,435 cm^{-1} was very noisy. Calibration functions were calculated for all four peaks visible in the spectra (1,515, 1,495, 1,465, and 1,379 cm^{-1}). They are shown in **Figure 4**. For each of these peaks, the LOD was calculated as the concentration where the signal was three times as high as the RMS noise of a 100% line of the solvent in the spectral region (1), according to:

$$LOD = \frac{3\sigma}{k} \qquad (1)$$

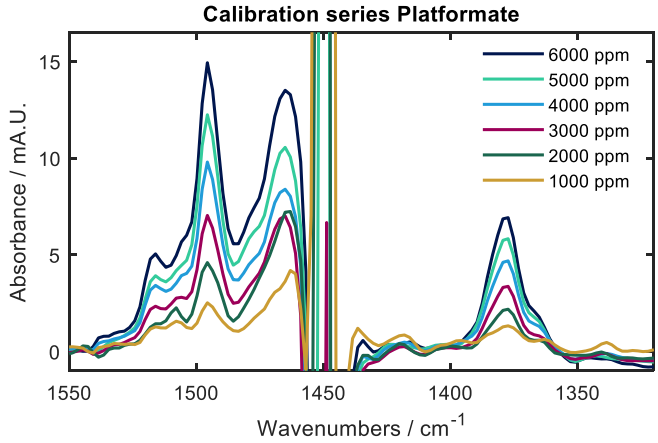

Figure 3: Influence of the concentration on the FTIR spectrum. Samples were dissolved in cyclohexane, causing noisy signal between 1,480 and 1,435 cm^{-1}, due to the high absorption of the CH_2 scissoring deformation vibration in this spectral region.

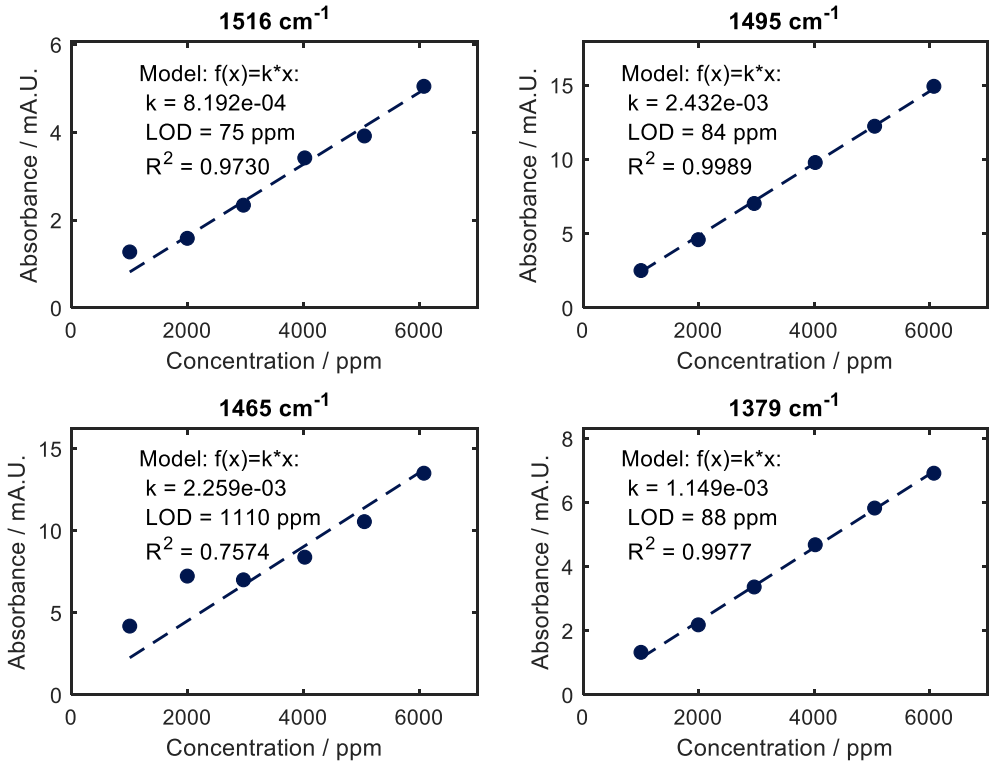

Figure 4: Calibration of the analyzer using the four bands seen in Figure 3, the 1,516 and 1,495 cm^{-1} bands attributed to C=C skeletal vibrations, the 1,465 cm^{-1} attributed to the asymmetric CH_3 deformation vibration, and the band at 1,379 cm^{-1} attributed to the symmetric CH_3 deformation vibration.

4.3.2. Use of the analyser for leak detection and quality control of petrochemical products

For the spectral determination of leaks in the pipelines in a petrochemical refinery, it is important to investigate the spectral differences exhibited by products at different points in the process. For the rectification of products after isomerization, this change can be seen in the region of the symmetric CH_3 deformation vibration, as already discussed in D3.2 for pure hydrocarbon samples. In **Figure 5**, this is demonstrated using hydrocarbon samples at three different points in the rectification column after the isomerization process. As can be seen for the three

spectra, the difference in branching leads to easily distinguishable spectra, with high percentage of branched product in the light top fraction, and the least amount of branched product in the bottom fraction, which can be also seen in the shift of the peak at 1,380 cm^{-1}.

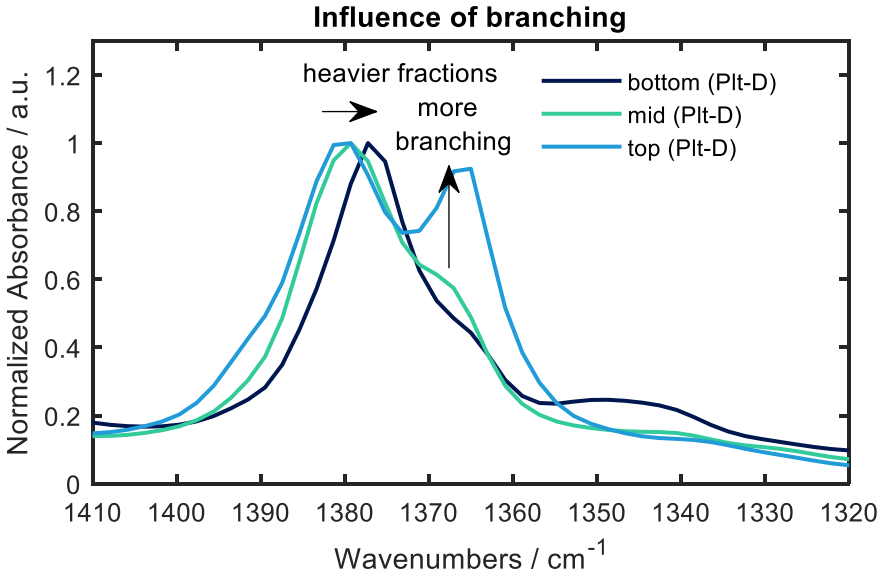

Figure 5: Influence of branching on the symmetric CH_3 deformation vibration. Samples were taken at different locations of a rectification column.

The influence of the different branching percentage and chain length can also be seen when comparing the two fractions being mixed to the isomerized product. In **Figure 6**, these spectral differences are displayed for the symmetric CH_3 deformation vibration region (top) and the combined CH_2 scissoring vibration/symmetric CH_3 deformation vibration region (bottom). Here, the infrared spectra are aligned with the expected results for the chosen mixture ratios, both with different CH_3 contents (both in quantity and branching for the heavier fraction, as can be seen in the top image in **Figure 6**) and the difference in CH_2 content for the less branched and heavier fraction, causing a shift in the combined CH_2 scissoring vibration/symmetric CH_3 deformation vibration peak for the isomerized product.

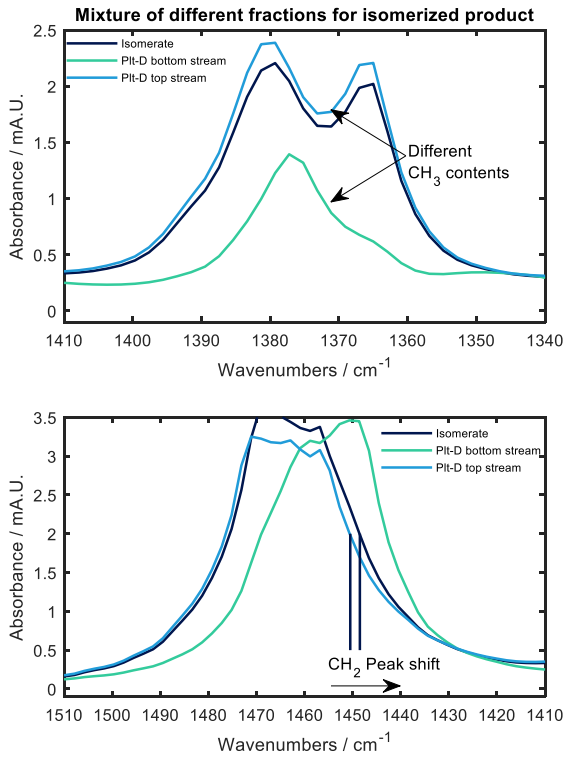

Figure 6: Spectral differences of the fractions obtained after isomerization and rectification (Plt-D bottom stream and Plt-D top stream) to the isomerised product (Isomerate). Top figure shows the difference in CH_3 contents for the heavier, unbranched Plt-D bottom stream fraction and the lighter, branched Plt-D top stream fraction compared to the isomerised product, while the bottom figure shows a peak shift for the fractions and the isomerised product in the CH_2 scissoring region.

Another very pronounced spectral feature can be observed for products with high aromatic hydrocarbon contents. This is demonstrated in **Figure 7**, where an aromatic-rich phase (~70% aromatic compounds) is compared to an aliphatic-rich phase (< 5% aromatic compounds). In this case, the presence of peaks attributed to the C=C skeletal vibrations can be seen clearly, further helping potentially identify the source of the leakage.

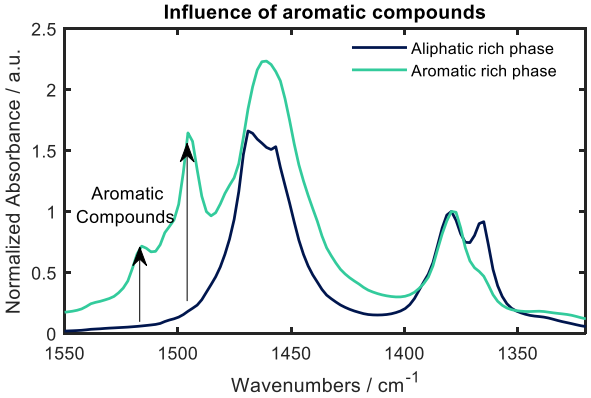

Figure 7: Influence of an aromatic-rich phase on the FTIR spectrum with the C=C skeletal vibrations at 1,495 and 1,517 cm^{-1}. Spectra were normalized to the absorbance signal of the symmetric CH_3 vibration at 1,380-1,375cm^{-1}.

It was found that another interesting application of the analyzer was the distinction of products from different plants. This is possible due to process parameter differences or different feeds, which can sometimes lead to a distinct fingerprint of certain plants. Such a phenomenon was encountered in the pilot phase and is exemplified in **Figure 8**, where the infrared spectra of the heavy naphtha products stemming from three different plants (Plt-A, Plt-B, Plt-C) are shown. No striking differences can be seen in the absorption bands of the symmetric CH_3 vibrations, highlighting similar plant performances. However, the higher aromatic content in the product stemming from Plt-B could hint at different feeds. In case any unwanted/unexpected changes in products happen, it could be shown hereby that the analyzer can serve as a quality control tool to quickly detect differences in the product. On the other hand, similar spectral features can hint at consistent quality, as can be seen in **Figure 9** for the diesel products stemming from the same three plants.

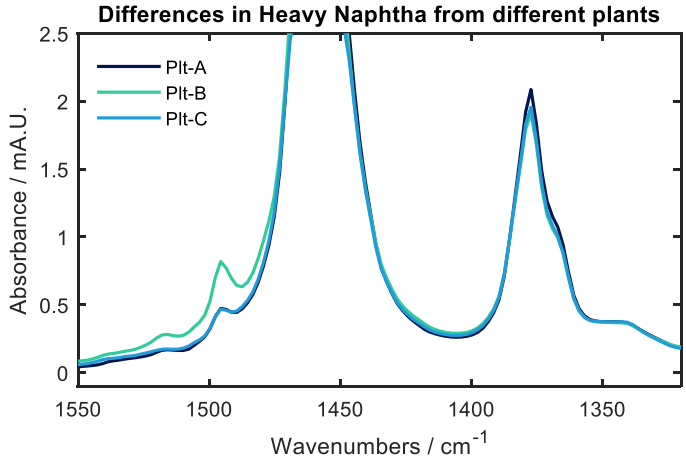

Figure 8: Influences of different production plants on the quality and chemical composition of heavy naphtha product. The spectrum was scaled to maximize the signal for the specific symmetric CH_3 deformation vibration and potential aromatic compounds.

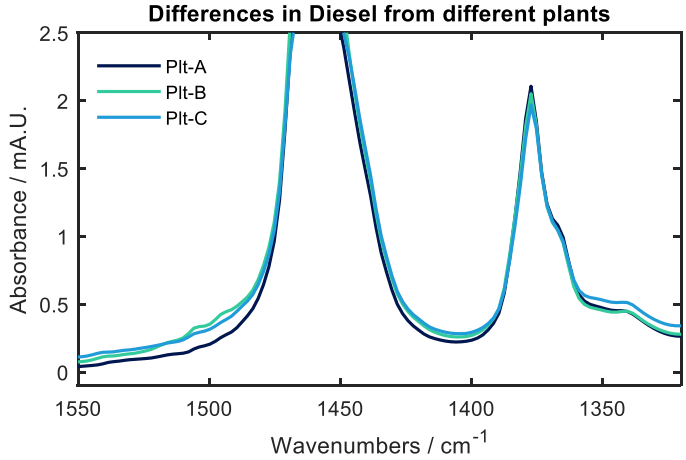

Figure 9: Influences of different production plants on the quality and chemical composition of diesel product. The spectrum was scaled to maximize the signal for the specific symmetric CH_3 deformation vibration and potential aromatic compounds.

Finally, potential differences in fractions and products from the same plant were investigated. For this purpose, light naphtha, heavy naphtha, as well as diesel and kerosene products were measured with the analyzer. The spectral results are shown in **Figure 10**. For these products, no significant amount of aromatic compounds could be detected, hence, we focused on their symmetric CH_3 deformation vibrations. For the light naphtha, a shift, hinting at more branching, and consistent with observations on lighter fractions, was observed, while the spectral

signatures of the remaining products were quite similar, with slight differences in the branching noticeable when comparing the peak shoulders around 1,365 cm^{-1}.

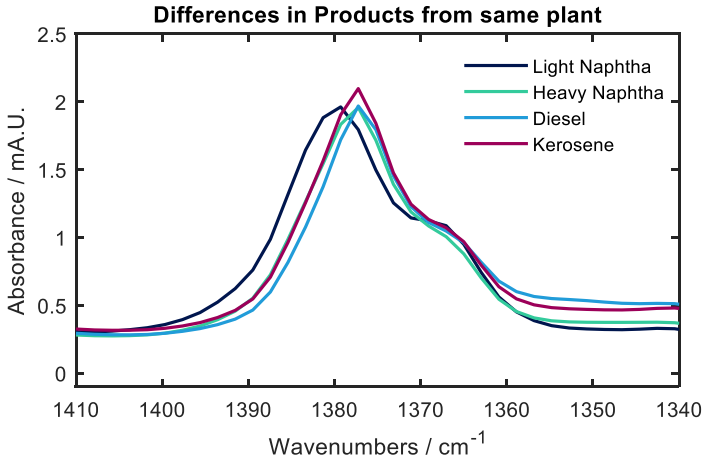

Figure 10: Spectral differences for the symmetric CH_3 deformation vibrations of different products produced at the same plant.

4.3.3. Using machine learning for estimating the origin of leaks

Tunable laser sources for the identification of different products in the petrochemical industry were developed in the HYDROPTICS project. Due to fabrication delays, they were not included in the final prototype, with a traditional FTIR being used instead. To simulate the information that could have been gained, the two spectral regions of interest as specified in D3.2 (shown in **Figure 11**) were used for further analysis.

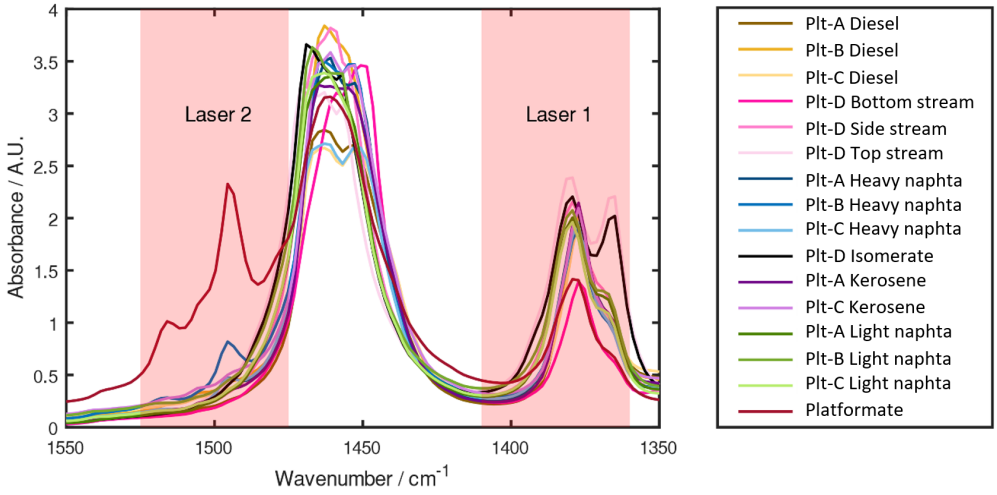

Figure 11: Spectra of the samples acquired in the second pilot with the spectral regions of interest (as specified in D3.2) marked in red.

Machine learning is a very potent tool for extracting more information of spectra which seem very similar at first glance. To demonstrate the possible impact of machine learning for the evaluation of spectral data in leak detection or quality control, principal component analysis (PCA) using a singular value decomposition (SVD) algorithm was performed for each spectral region, as well as the whole spectral dataset. The results of this data analysis are shown in **Figure 12-Figure 14**. Most products could be very clearly discriminated, showing the high potential of an on-line device for the rapid screening of cooling water.

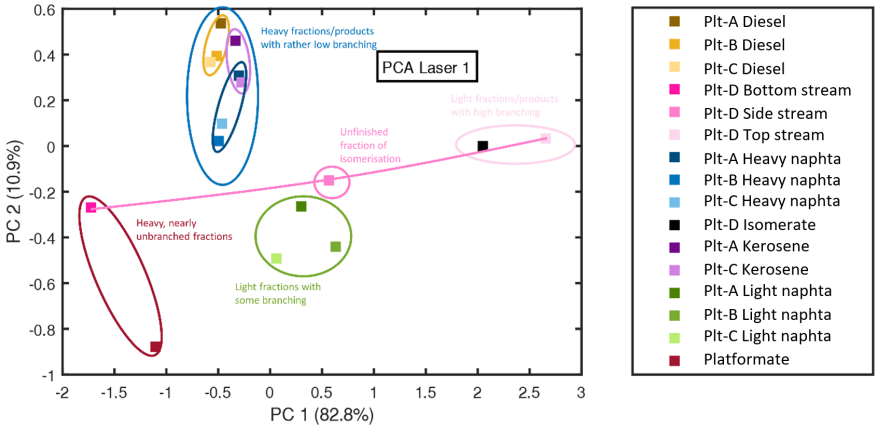

Figure 12: PCA of the spectral features in the first region of interest (branching and chain length).

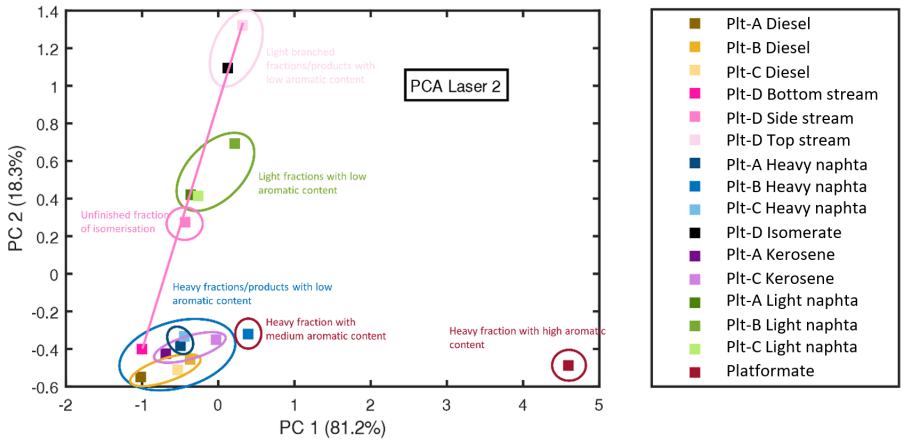

Figure 13: PCA of the second spectral region of interest (aromatic content and chain length).

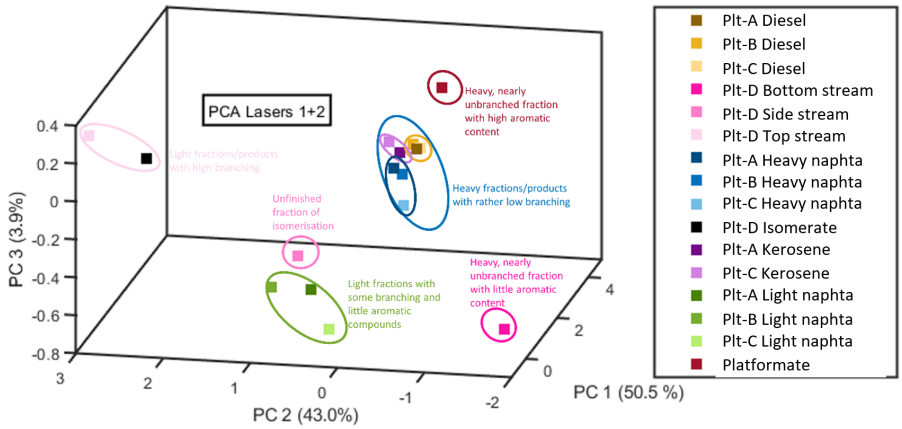

Figure 14: PCA of the full spectral information in both regions of interest (branching, aromatic content, and chain length).

5. Conclusions

In summary, the capability of an IR-based at-line analyzer to identify and deliver information on oil leaks in a refinery was demonstrated at the premises of TUPRAS in the frame of the Pilot II phase. For this purpose, the two spectral regions defined in the early stages of the project (1,360-1,410 cm^{-1} and 1,470-1,520 cm^{-1}) revealed valuable information on the type of products measured. An LOD of ~80 ppm in Cyclohexane was measured, which would

equate to an LOD of 5 ppm in OiW, considering an extraction factor of 18. The potential improvement steps may include adaptation of the analyzer to sudden changes in the oil content, as the oil content is variable due to leaks in the process. At the current stage, recalibration is required when the oil content in the sample accumulated and there was a deviation from the nominal value.

Overall, the capabilities of on-line OiW analysis, as demonstrated in the Pilot I phase, coupled with tunable infrared spectroscopy, as demonstrated in this Pilot II phase, may be used to quickly identify, and react to leaks in cooling water systems, significantly reducing down-time and improving efficiency.

6. Abbreviations

Abbreviation	Meaning
OiW	Oil in water
LOD	Limit of detection
PCA	Principal component analysis
SVD	Singular value decomposition